






# Precise Orbit Determination of CubeSats Using Proposed Observations Weighting Model

Amir Allahviridi-Zadeh , Ahmed El-Mowafy , and Kan Wang 

## Abstract

CubeSats can be used for many space missions and Earth science applications if their orbits can be determined precisely. The Precise Orbit Determination (POD) methods are well developed for large LEO satellites during the last two decades. However, CubeSats are built from Commercial Off-The-Shelf (COTS) components and have their own characteristics, which need more investigations. In this paper, precise orbits of 17 3U-CubeSats in the Spire Global constellation are determined using both the reduced-dynamic and the kinematic POD methods. The limitations in using elevation-dependent weighting models for CubeSats POD are also discussed and, as an alternative approach, a weighting model based on the Signal-to-Noise Ratio (SNR) has been proposed. One-month processing of these CubeSats revealed that around 40% of orbits can be determined at the decimeter accuracy, while 50% have accuracy at centimeters. Such precise orbits fulfil most mission requirements that require such POD accuracy. Internal validation methods confirmed the POD procedure and approved the distinction of weighting based on SNR values over the elevation angles.

## Keywords

CubeSats · Precise orbit determination (POD) · Signal-to-noise ratio (SNR) · Weighting model

## 1 Introduction

CubeSats are small low-cost and low-power satellites that can be used for many space missions. Precise Orbit Determination (POD) of CubeSats is essential for some missions such as radio-occultation, Interferometric Synthetic Aperture Radar (InSAR), satellite altimetry, gravity field recovery, and future mega-constellations as an augmentation system for positioning and navigation (Allahviridi-Zadeh and El-

Mowafy 2022). POD of CubeSats using the observations of Global Navigation Satellite Systems (GNSS) can be performed using the reduced-dynamic and the kinematic methods in post-mission or real-time (Allahviridi-Zadeh et al. 2022a). In this study, we analyze the POD of CubeSats from the Spire CubeSat Constellation (Spire Global, Inc.), comparing elevation angle-dependent and Signal-to-Noise ratio (SNR) based weighting models.

The Spire Global constellation of nanosatellites consists of more than 145 3U-CubeSats ( $10 \times 10 \times 30$  cm) that were launched mostly in Sun-synchronous and various other orbits with different altitudes (445–600 km). Most are equipped with the STRATOS GNSS receiver module to receive 1-Hz dual-frequency GPS signals (L1C/A and L2L) using a compatible zenith-mounted GNSS antenna. It also simultaneously collects 50-Hz signals dual-frequency multi-GNSS signals through the high-gain, side-mounted antennas from setting or rising GNSS satellites to perform Radio Occul-

A. Allahviridi-Zadeh (✉) · A. El-Mowafy  
GNSS-SPAN Group, School of Earth and Planetary Sciences, Curtin  
University, Perth, Australia  
e-mail: [amir.allahviridizadeh@curtin.edu.au](mailto:amir.allahviridizadeh@curtin.edu.au)

K. Wang  
National Time Service Center, Chinese Academy of Sciences, Xi'an,  
China

University of Chinese Academy of Sciences, Beijing, China

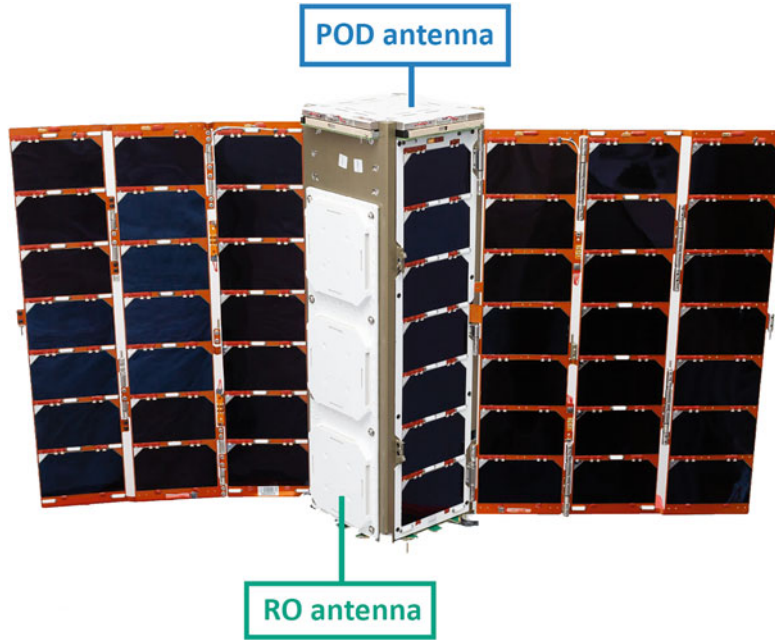


**Fig. 1** Structure of the Spire 3U RO CubeSat (Credit: Spire Global, Inc.)

tation (RO). The location of the POD and RO high-gain antennas on the Spire’s CubeSats are depicted in Fig. 1.

## 2 Precise Orbit Determination

The reduced-dynamic POD (RD-POD) is considered the main method in this study. It is based on exploiting available dynamic models as well as GNSS observations to estimate the CubeSat’s state vector, which includes position and velocity, clock offsets, float ambiguities, and some piece-wise constant stochastic accelerations to compensate for deficiencies in dynamic models (Allahviridi-Zadeh et al. 2022a). The type of data used, processing information, and models in the RD-POD processing are provided in Table 1.

### 2.1 Weighting Models

Equal weighting of GNSS observations can be considered for the POD of Low Earth Orbit (LEO) satellites. However, this model is not optimal due to factors causing mis-modelled errors, such as higher-order ionosphere scintillation, near field multipath, etc. One may suggest using the elevation-angle dependent (defined here for brevity as elevation-dependent) weighting models such as  $\sin^2\theta$ . The analysis of the observation residuals in the validation step (see Sect. 2.3.3) reveals that this type of models is not optimal for reflecting the actual noise level of the CubeSats observations. This is due to the fact that these models

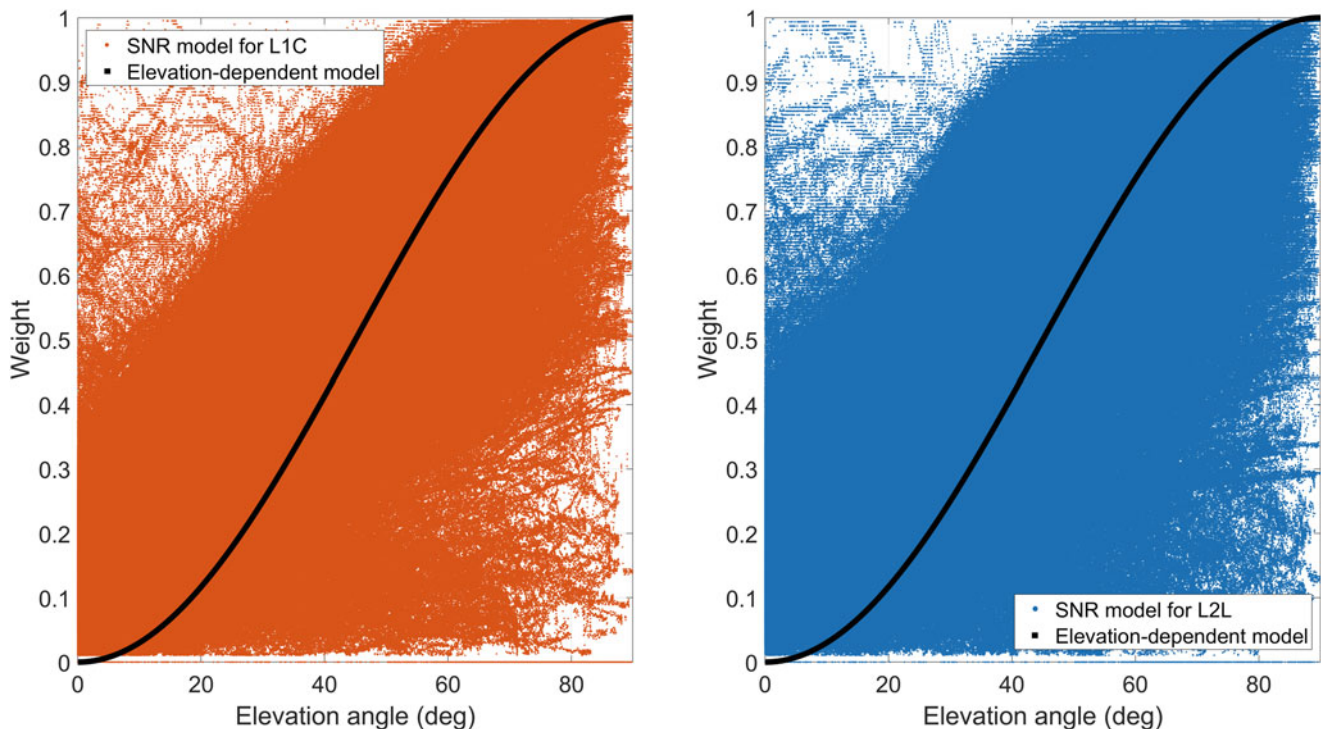
are developed to account for the effect of the tropospheric delays and multipath, mainly for users on the Earth surface (Hobiger and Jakowski 2017), whereas CubeSats fly above the troposphere layer. Besides, in order to correctly apply the elevation-dependent model, the CubeSat should effectively record the attitude information, such as the quaternions. This, however, may not be available for CubeSats with low-power budget. Hence, we propose to use a direct signal quality indicator, i.e. the SNR, which equals to the ratio of the signal power to the noise power of the modulated signal at the correlator output. The proposed SNR-based model for weighting the observations ( $\Phi_i$ ) can be expressed as:

$$W(\Phi_i) = \left( 0.1 + 0.9 * \left( \frac{\Delta SNR_{i,min}}{\Delta SNR_{max,min}} \right) \right)^2 \quad (1)$$

where  $\Delta SNR_{i,min}$  is the difference between the observation SNR value and the minimum SNR of all observations, and  $\Delta SNR_{max,min}$  is the difference between the maximum and minimum SNR values among all observations. The coefficients 0.1 and 0.9 on the right-hand side of Eq. 1 are used to give the maximum weight, i.e., 1, to the observation which has the highest SNR value, and a very low weight, i.e., 0.01, to the observation with the lowest SNR. A similar model has been developed for baseline processing (Luo 2013), however, the way of choosing the maximum and minimum SNR values and applying weights for double differences are different. Figure 2 compares the weights generated from applying the elevation-dependent weighting model ( $\sin^2\theta$ ) and the SNR-based model (Eq. 1) for different elevation angles ( $\theta$ ) for one-month observations of CubeSat PRN099. Two

**Table 1** CubeSats POD processing models and parameters

Item	Description
Gravity field/Earth tide/Relativity/Other planets	EGM 2008 (Pavlis et al. 2008)/FES2004 (Lyard et al. 2006)/IERS 2010 (Petit and Luzum 2010)/DE405 (Standish 1998)
Observation model	1-Hz dual-frequency GPS Ionosphere-Free
A-priori code and phase standard deviation	0.1 m, 1 mm (Zenith, L1)
Empirical acceleration	piece-wise constant accelerations
Attitude information, Quaternions, Antenna phase center offsets (PCO) and variations (PCV)	Provided by Spire Global, Inc. and applied (Allahviridi-Zadeh 2021b)
Weighting model (tested)	Elevation-dependent or SNR-based models
GNSS orbits and clocks	IGS-RTS and CODE final

**Fig. 2** Observation weights from the SNR- and the elevation-dependent weighting models for one month (16/12/2020–15/01/2021) of L1C (left) and L2L (right) signals from all available GPS satellites as observed on CubeSat PRN099

models behave differently in weighting the observations. For example, the SNR-based model gives higher weights to the observations from low elevation angles for both L1C and L2L signals compared with the elevation-dependent model depending on the received signal strength. It can be more realistic for signals in space, since they are not affected by the troposphere, and the amount of near-field multipath is low, mainly due to the CubeSat structure (see Fig. 1). Realistic weighting is crucial in the POD of the low-power CubeSats since they are allowed to record the observations for a limited time based on their power budget and mission requirements (personal communication with the CubeSat developers (Allahviridi-Zadeh 2021a)). Therefore, losing observations due to incorrect weighting may even lead to the unavailability of POD procedure for the Kinematic mode. It does not generally though take place for the satellites that

record GNSS observations continuously, since the RD-POD of these satellites can run even in the presence of duty-cycled GNSS data (i.e., available at certain percentage of the orbit due to the need of the low available onboard power to sensors other than GNSS) (Wang et al. 2020).

## 2.2 POD Results

One month (from 16 December 2020 to 15 January 2021) of all available observations of 17 3U-CubeSats from the Spire Global constellation are processed in this study. A list of these CubeSats and their specifications are given in Allahviridi-Zadeh et al. 2022b. The observations comprise several segments each day. Each segment has around 1.5 h (orbital period) of 1-Hz dual-frequency GPS data. The

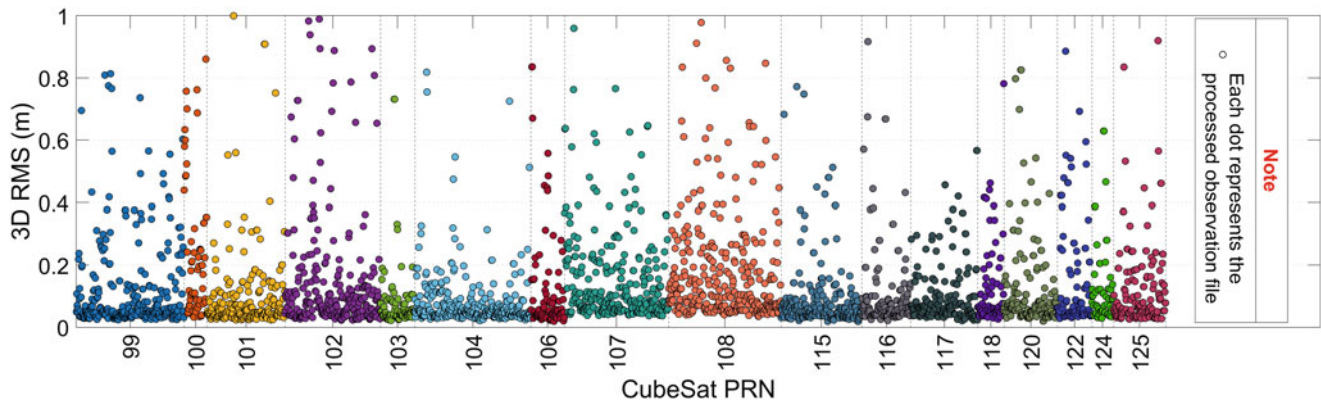


**Fig. 3** 3D-RMS of differences between RD-POD and Kinematic POD (Kin-POD) for all CubeSats. Each segment related to each CubeSat PRN contains all processed file during one month (16/12/2020–15/01/2021)

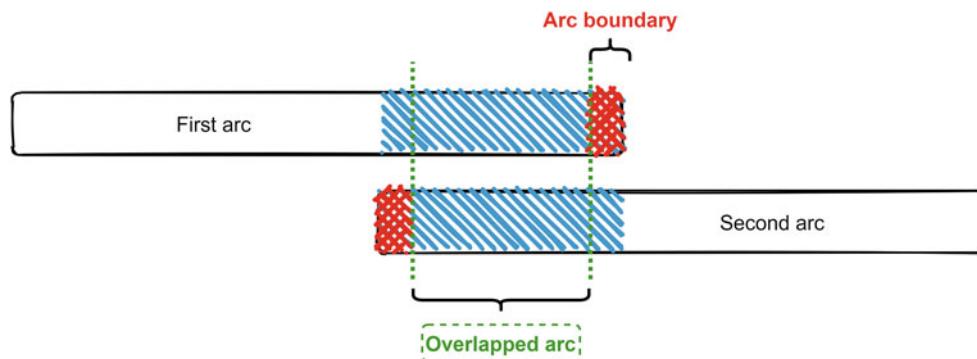


**Fig. 4** Overlapped arc between two consecutive orbits. The red cross hatches indicate the arc boundaries

related observable-specific signal biases for L1C and L2L are synchronized with the applied precise GNSS orbits and clocks (Schaer 2016). A comparison between the reduced-dynamic orbits, as the most precise obtainable orbits in this study, and the kinematic orbits are plotted in Fig. 3 in the radial (R), along-track (S), and cross-track (W) directions. In this comparison, 40% of kinematic orbits have 3D root mean square (3D-RMS) of decimeters, while half of them have accuracies at a few centimeters. Such orbits can fulfil the requirements of different space missions and earth-science applications such as radio occultation, InSAR, the Earth monitoring, etc. (Allahviridi-Zadeh et al. 2021).

## 2.3 POD Validation

The Spire CubeSats are not equipped with Satellite Laser Ranging (SLR) reflectors, and thus, external validation is not possible. Therefore, the internal methods including the overlapping arcs, residuals analysis, and goodness of fit checks are used to validate the POD results. Their results are described in the following sections.

### 2.3.1 Overlapping Arcs

The overlapping validation is performed by testing two consecutive arcs longer than 24 h (e.g. 30 h) and checking the differences in the overlapped part. The estimated CubeSats orbits are all around 1.5 h arcs due to the length of the observation segments. All possible overlapped arcs between all estimated orbits of each CubeSat, except for the arc boundaries, are considered for this validation method. Figure 4 shows a sample of the overlapped arc between two consecutive orbits.

The RMS of the overlapped differences for RD-POD and Kinematic POD (Kin-POD) in all directions are plotted in Fig. 5. Small RMS values indicate validation of the POD procedure. The overall average reduction in RMS for the Kin-POD, are also observed when using the SNR-based weighting (dark colours) against the elevation-dependent model (light colours). This confirms the benefits of using the SNR-based model for the CubeSat's kinematic POD. The average percentage of the RMS reduction for all CubeSats are provided in Table 2. In the RD-POD, the overlapping results applying both models are similar. This could be

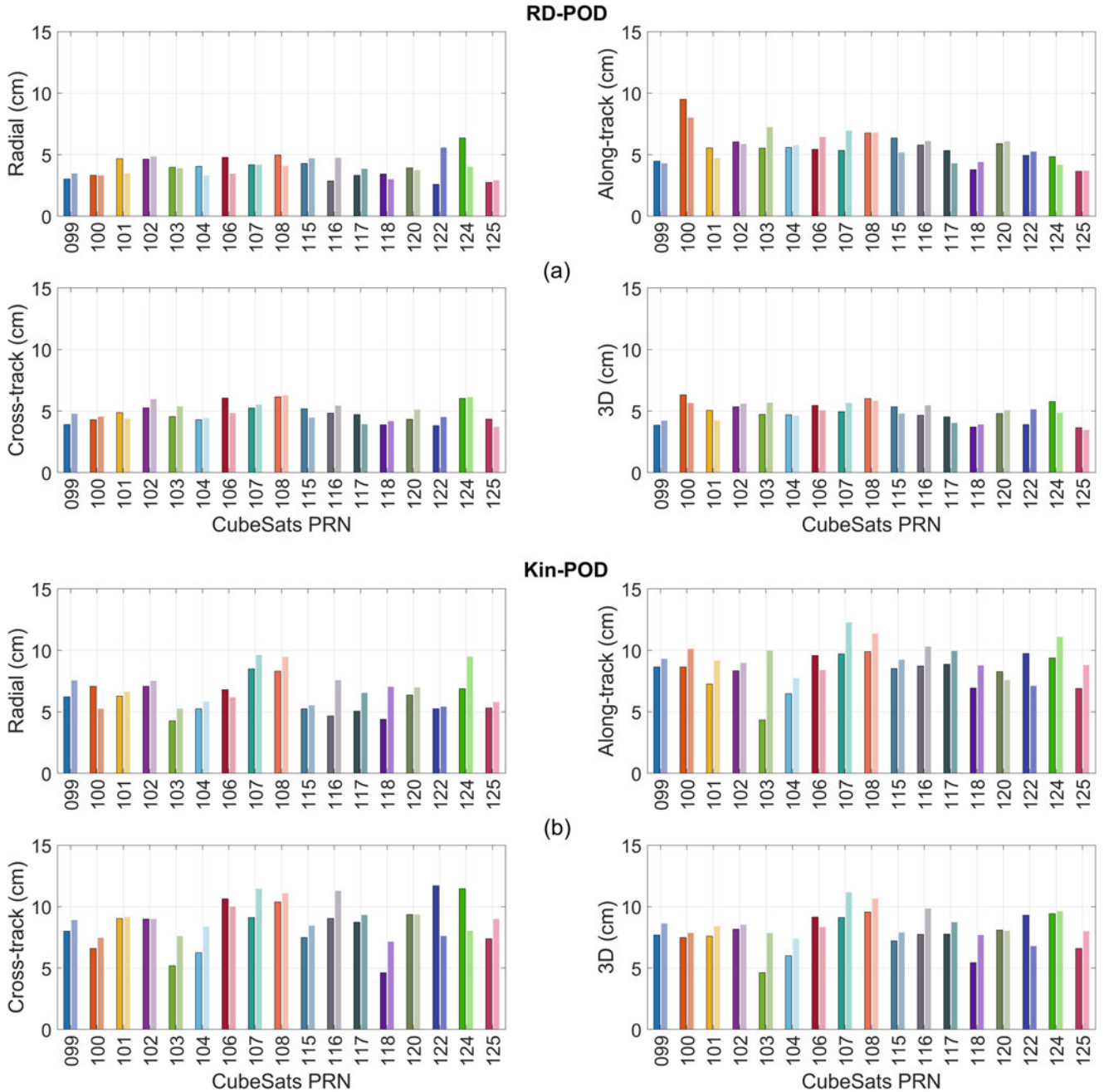


**Fig. 5** RMS of overlapping validation for RD-POD (a) and Kin-POD (b). (Dark colours: using the SNR-based model – Light colours: using the elevation-dependent model)

due to the impact of using similar dynamic models and estimating the piecewise accelerations in the RD-POD using both weighting models.

### 2.3.2 Goodness of Fit

The a-posteriori variance can be expressed as:

$$\hat{\sigma}_0^2 = \frac{\|\hat{e}\|_W^2}{dof}$$

(2) where  $\left(\|\hat{e}\|_W^2 = \hat{e}^T W \hat{e}\right)$  is the weighted squared norm of the observation residuals ( $\hat{e}$ ) using the observation weight

**Table 2** Mean percentage of the RMS reduction due to the proposed SNR-based model compared to the elevation-dependent model for all CubeSats in all directions

POD	Radial (%)	Along-Track (%)	Cross-Track (%)	3D (%)
RD	<b>0.0</b>	<b>0.1</b>	<b>0.0</b>	<b>0.1</b>
Kin	<b>11.2</b>	<b>11.1</b>	<b>5.7</b>	<b>9.5</b>

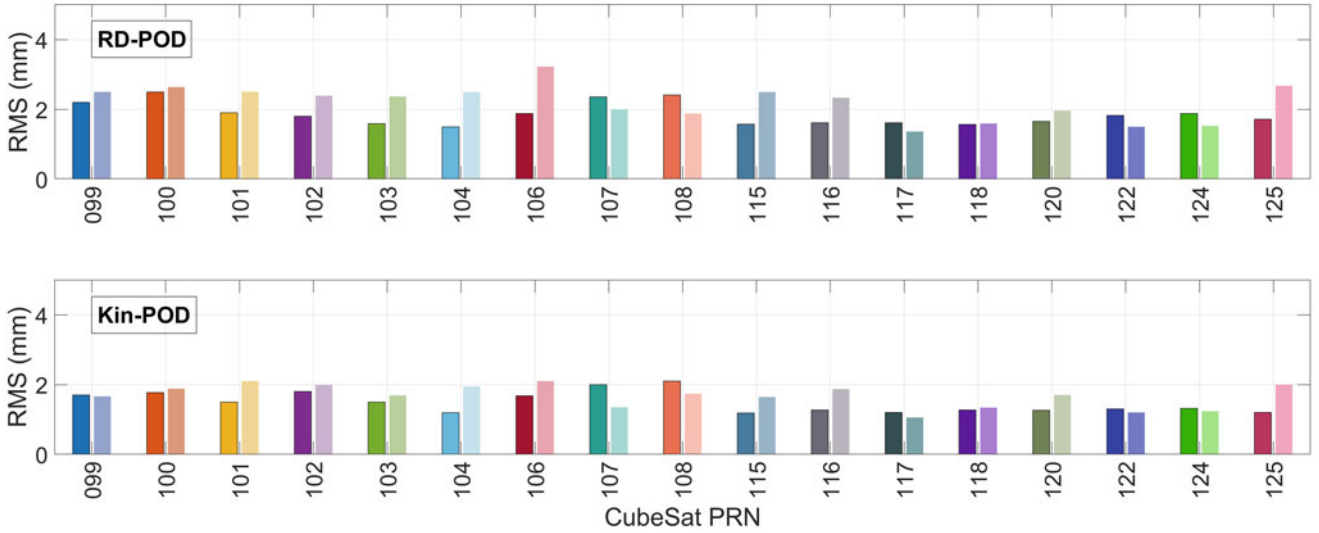


**Fig. 6** RMS of the a-posteriori sigma for all CubeSats for RD-POD (top) and Kin-POD (bottom). (Dark colours: using the SNR-based model—Light colours: using the elevation-dependent model)

**Table 3** Mean value of the a-posteriori STD of all CubeSats from RD-POD and Kin-POD

POD	Mean value of the a-posteriori sigma (mm)	
	SNR-based model	Elevation-dependent model
RD	1.85	2.20
Kin	1.48	1.67

matrix ( $W$ ) and  $dof$  denotes the degrees of freedom. The ratio of a-posteriori variance to the a-priori variance (see Table 1) can be used as a self-consistency check of the goodness of fit using the following chi-squared test with selected confidence region ( $\alpha$ ) (Strang and Borre 1997):

$$\frac{\hat{\sigma}_0^2}{\sigma_0^s} < \frac{\chi_{dof,1-\alpha}^2}{dof} \quad (3)$$

The a-posteriori standard deviation (STD) values of all CubeSats are plotted in Fig. 6. They are all less than 3 mm which represents an acceptable fitting model to the POD problem. The mean of all a-posteriori STD values for all tested CubeSats are given in Table 3. In total, 16% and 11% reduction in the a-posteriori STD values are observed in the case of POD using SNR-based weighting model for RD-POD and Kin-POD, respectively.

### 2.3.3 Residual Analysis

The final validation check is the observation residual analysis. As a representative example, the GPS ionosphere-free (IF) phase residuals for CubeSat PRN-099 are plotted in Fig. 7. The ambiguities were estimated as float values in our POD processing. The residuals are at sub-centimeter to centimeter

level mainly due to the onboard COTS receiver/antenna, as well as using the IF-LC which increases the noise compared to the use of uncombined signals. However, the reduction of the residuals is obvious for the POD using the SNR-based model. Similar trends are observed for other CubeSats.

The CubeSats cross the eclipse region several times per day. Although the solar radiation pressure is significantly low due to the absence of sunlight, there is a thermal re-radiation as an additional effect of the solar radiation pressure in these regions (Švehla 2018). A cylindrical model proposed by Allahviridi-Zadeh (2013, 2022) and Allahverdi-Zadeh et al. (2016) is used to estimate the eclipse region and analyse the residual behaviours. No significant changes on residuals can be observed for crossing this region. The reason is that such effect has been captured by the estimation of stochastic accelerations in the POD procedure.

## 3 Conclusion

The proposed SNR-based weighting model reduced the IF phase residuals compared to the traditional elevation angle-dependent model. The internal validation including comparing overlapping arcs and the a-posteriori STD confirmed the improved performance of CubeSats' POD using the proposed SNR-based weighting model. The generated CubeSats orbits have a precision that fulfils the requirements of different space and Earth science applications. The impact of using such a weighting model on ambiguity resolution is among our next studies.

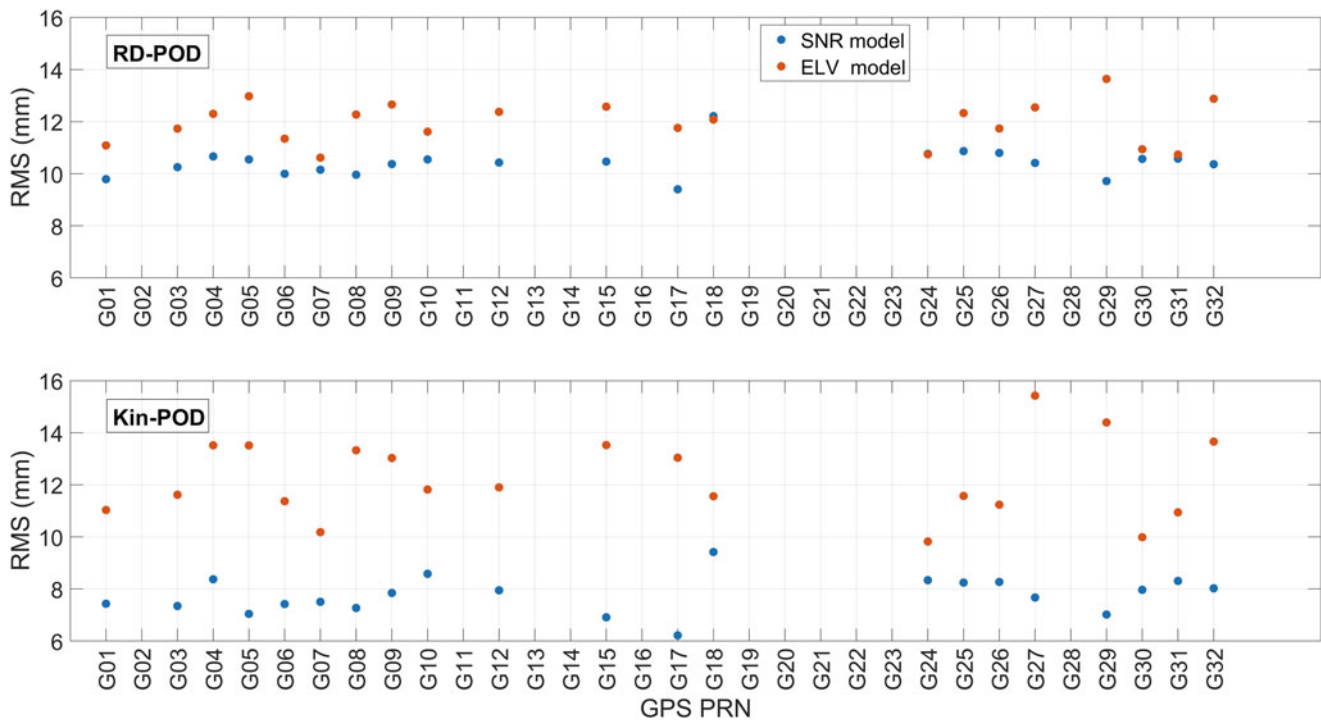


**Fig. 7** The RMS of IF phase residuals from the RD-POD (top) and the Kin-POD (bottom) for CubeSat PRN099. The RMS values are derived from one month of all observations of all GPS satellites

**Acknowledgments** We would like to thank Spire Global, Inc for providing the nanosatellite data for scientific research. Special thanks to Dallas Masters, Ph.D., Director of Earth observations/GNSS and his team for our discussions on the satellite structure and for providing the required information. This work is funded by the Australian Research Council under the discovery project “Tracking Formation-Flying of Nanosatellites Using Inter-Satellite Links” (DP 190102444). Third author receives fund from the Chinese Academy of Science (CAS) “Light of West China” Program (No. XAB2018YDYLO1).

## References

- Allahverdi-Zadeh A, Asgari J, Amiri-Simkooei AR (2016) Investigation of GPS draconitic year effect on GPS time series of eliminated eclipsing GPS satellite data. *J Geod Sci* 6. <https://doi.org/10.1515/jogs-2016-0007>
- Allahverdi-Zadeh A (2013) Evaluation of the GPS observable effects located in the earth shadow on permanent station position time series. MSc thesis, Geomatics Engineering Department, University of Isfahan. <https://doi.org/10.13140/RG.2.2.28151.32167>
- Allahverdi-Zadeh A (2021a) Software Defined Radio (SDR) as a GNSS receiver in future CubeSats. In: Internship with Binar Space Program – Innovation Central Perth. Curtin University, Perth, Western Australia. <https://doi.org/10.13140/RG.2.2.28290.20166>
- Allahverdi-Zadeh A (2021b) Phase centre variation of the GNSS antenna onboard the CubeSats and its impact on precise orbit determination. In: Proceedings of the GSA Earth Sciences Student Symposium, Western Australia (GESSS-WA), Perth, Australia, 25 November 2021. <https://doi.org/10.13140/RG.2.2.10355.45607/1>
- Allahverdi-Zadeh A, Wang K, El-Mowafy A (2021) POD of small LEO satellites based on precise real-time MADOCA and SBAS-aided PPP corrections. *GPS Solut* 25:31. <https://doi.org/10.1007/s10291-020-01078-8>
- Allahverdi-Zadeh A (2022) Shadow toolbox. figshare. Software. <https://doi.org/10.6084/m9.figshare.19085546.v1>
- Allahverdi-Zadeh A, El-Mowafy A (2022) The impact of precise inter-satellite ranges on relative precise orbit determination in a smart CubeSats constellation, EGU General Assembly 2022, Vienna, Austria, 23–27 May 2022, EGU22-2215, <https://doi.org/10.5194/egusphere-egu22-2215>
- Allahverdi-Zadeh A, Wang K, El-Mowafy A (2022a) Precise orbit determination of LEO satellites based on undifferenced GNSS observations. *J Surv Eng* 148:03121001. [https://doi.org/10.1061/\(ASCE\)SU.1943-5428.0000382](https://doi.org/10.1061/(ASCE)SU.1943-5428.0000382)
- Allahverdi-Zadeh A, Awange J, El-Mowafy A, Ding T, Wang K (2022b) Stability of CubeSat clocks and their impacts on GNSS radio occultation. *Remote Sens* 14:362. <https://doi.org/10.3390/rs14020362>
- Hobiger T, Jakowski N (2017) Atmospheric signal propagation. In: Teunissen PJG, Montenbruck O (eds) Springer handbook of global navigation satellite systems. Springer International Publishing, Cham, pp 165–193. [https://doi.org/10.1007/978-3-319-42928-1\\_6](https://doi.org/10.1007/978-3-319-42928-1_6)
- Luo X (2013) Observation weighting using signal quality measures. In: GPS stochastic modelling: signal quality measures and ARMA processes. Springer, Berlin, pp 137–162. [https://doi.org/10.1007/978-3-642-34836-5\\_5](https://doi.org/10.1007/978-3-642-34836-5_5)
- Lyard F, Lefevre F, Letellier T, Francis O (2006) Modelling the global ocean tides: modern insights from FES2004. *Ocean Dyn* 56:394–415. <https://doi.org/10.1007/s10236-006-0086-x>
- Pavlis N, Kenyon S, Factor J, Holmes S (2008) Earth gravitational model 2008. In: SEG technical program expanded abstracts 2008. SEG technical program expanded abstracts. Society of Exploration Geophysicists, pp 761–763. <https://doi.org/10.1190/1.3063757>
- Petit G, Luzum B (2010) IERS conventions. (IERS Technical Note; 36) Frankfurt am Main: Verlag des Bundesamts für Kartographie und Geodäsie, p 179. ISBN 3-89888-989-6
- Schaer S (2016) SINEX BIAS—Solution (Software/technique) Independent Exchange Format for GNSS BIASes Version 1.00. In: IGS

- workshop on GNSS biases, Bern, Switzerland. [http://ftp.aiub.unibe.ch/bcwg/format/sinex\\_bias\\_100.pdf](http://ftp.aiub.unibe.ch/bcwg/format/sinex_bias_100.pdf)
- Spire Global Inc. <https://spire.com/>. Accessed 13 August 2021
- Strang G, Borre K (1997) Linear algebra, geodesy, and GPS. Wellesley-Cambridge Press
- Švehla D (2018) Geometrical theory of satellite orbits and gravity field. Springer, Online. <https://doi.org/10.1007/978-3-319-76873-1>
- Wang K, Allahviridi-Zadeh A, El-Mowafy A, Gross JN (2020) A sensitivity study of POD using dual-frequency GPS for cubesats data limitation and resources. Remote Sens 12(13):2107. <https://doi.org/10.3390/rs12132107>

**Open Access** This chapter is licensed under the terms of the Creative Commons Attribution 4.0 International License (<http://creativecommons.org/licenses/by/4.0/>), which permits use, sharing, adaptation, distribution and reproduction in any medium or format, as long as you give appropriate credit to the original author(s) and the source, provide a link to the Creative Commons license and indicate if changes were made.

The images or other third party material in this chapter are included in the chapter's Creative Commons license, unless indicated otherwise in a credit line to the material. If material is not included in the chapter's Creative Commons license and your intended use is not permitted by statutory regulation or exceeds the permitted use, you will need to obtain permission directly from the copyright holder.

